JCI The Journal of Clinical Investigation

Targeted *p16^{Ink4a}* epimutation causes tumorigenesis and reduces survival in mice

Da-Hai Yu, Robert A. Waterland, Pumin Zhang, Deborah Schady, Miao-Hsueh Chen, Yongtao Guan, Manasi Gadkari, Lanlan Shen

J Clin Invest. 2014;124(9):3708-3712. https://doi.org/10.1172/JCI76507.

Brief Report Oncology

Cancer has long been viewed as a genetic disease; however, epigenetic silencing as the result of aberrant promoter DNA methylation is frequently associated with cancer development, suggesting an epigenetic component to the disease. Nonetheless, it has remained unclear whether an epimutation (an aberrant change in epigenetic regulation) can induce tumorigenesis. Here, we exploited a functionally validated *cis*-acting regulatory element and devised a strategy to induce developmentally regulated genomic targeting of DNA methylation. We used this system to target DNA methylation within the *p16^{Ink4a}* promoter in mice in vivo. Engineered*p16^{Ink4a}* promoter hypermethylation led to transcriptional suppression in somatic tissues during aging and increased the incidence of spontaneous cancers in these mice. Further, mice carrying a germline *p16^{Ink4a}* mutation in one allele and a somatic epimutation in the other had accelerated tumor onset and substantially shortened tumor-free survival. Taken together, these results provide direct functional evidence that *p16^{Ink4a}* epimutation drives tumor formation and malignant progression and validate a targeted methylation approach to epigenetic engineering.

Targeted *p16^{Ink4a}* epimutation causes tumorigenesis and reduces survival in mice

Da-Hai Yu,[1] Robert A. Waterland,[1,2] Pumin Zhang,[3] Deborah Schady,[4] Miao-Hsueh Chen,[1] Yongtao Guan,[1,2] Manasi Gadkari,[1] and Lanlan Shen[1]

[1]Department of Pediatrics, Baylor College of Medicine, USDA/ARS Children's Nutrition Research Center, Houston, Texas, USA. [2]Department of Molecular and Human Genetics, [3]Department of Molecular Physiology and Biophysics, and [4]Department of Pathology, Texas Children's Hospital, Baylor College of Medicine, Houston, Texas, USA.

Cancer has long been viewed as a genetic disease; however, epigenetic silencing as the result of aberrant promoter DNA methylation is frequently associated with cancer development, suggesting an epigenetic component to the disease. Nonetheless, it has remained unclear whether an epimutation (an aberrant change in epigenetic regulation) can induce tumorigenesis. Here, we exploited a functionally validated *cis*-acting regulatory element and devised a strategy to induce developmentally regulated genomic targeting of DNA methylation. We used this system to target DNA methylation within the *p16^{Ink4a}* promoter in mice in vivo. Engineered *p16^{Ink4a}* promoter hypermethylation led to transcriptional suppression in somatic tissues during aging and increased the incidence of spontaneous cancers in these mice. Further, mice carrying a germline *p16^{Ink4a}* mutation in one allele and a somatic epimutation in the other had accelerated tumor onset and substantially shortened tumor-free survival. Taken together, these results provide direct functional evidence that *p16^{Ink4a}* epimutation drives tumor formation and malignant progression and validate a targeted methylation approach to epigenetic engineering.

Introduction

More than 25 years ago, it was proposed that epimutation — mitotically stable gene silencing associated with epigenetic alteration in DNA methylation — can act as 1 of Knudson's 2 hits required for tumorigenesis (1). In subsequent decades, many promoter CpG island–associated (CGI-associated) genes have been shown to be aberrantly hypermethylated and silenced in various cancers (2). Indeed, recent epigenomic studies revealed that nearly all tumor types harbor hundreds of abnormally hypermethylated promoter CGIs (3), which indicates that epimutations are as common in tumors as genetic mutations. We and others have demonstrated that aberrant promoter CGI methylation is associated with distinct environmental exposures (4), gene mutation patterns (5), cancer prognosis (6), and response to therapy (7). Despite the undisputed importance of DNA methylation in cancer, however, its fundamental role in carcinogenesis remains unclear (8, 9). Most importantly, it remains unknown whether aberrant DNA methylation is a cause of tumorigenesis (8).

Cancer-related promoter CGI hypermethylation originates in normal tissues, which suggests that aberrant methylation could predispose to malignancy (10). *p16^{Ink4a}* (referred to hereafter as *p16*) is a tumor suppressor gene that regulates the ability of retinoblastoma protein to control exit from the G1 stage of the cell cycle (11). Inactivation of *p16* by promoter CGI methylation is among the most common and earliest epigenetic events in human cancer (12) and is frequently detected in preneoplastic lesions (13–15). Mice provide an apt model in which to study epigenetic dysregulation of *p16* in cancer; in a mouse model of chemically induced lung cancer, *p16* methylation is a very early event (16). Moreover, *p16* age-associated hypermethylation is observed in several normal human and mouse tissues (17–19). Together, these data suggest that epigenetic silencing of *p16* in aging cells facilitates early abnormal clonal expansion, driving tumorigenesis (20). Directly testing this hypothesis, however, requires the ability to specifically target methylation to the *p16* promoter CGI.

Results and Discussion

Because *cis*-acting DNA sequences are important for the establishment of genomic patterns of DNA methylation (21, 22), we set out to engineer a *cis* element to attract DNA methyltransferases during development to achieve targeted de novo DNA methylation in vivo. We built upon our recent demonstration that an exceptional class of promoter CGIs that are methylated and silenced in normal somatic tissues is associated with specific *cis*-acting DNA motifs (23). To test the function of the identified motifs in vitro, we constructed a 140-bp *cis* element containing the top 3 motifs in the order and orientation most frequently observed in the normally methylated CGIs (Supplemental Figure 1; supplemental material available online with this article; doi:10.1172/JCI76507DS1). We used a stable integrated system to test transgenes targeting 2 human promoter CGIs, one at *INSL6* and another at *p16*, for 80 days in cell culture using both human (LNCaP) and mouse (NIH3T3) cell lines. The *cis* element induced extensive and progressive de novo methylation throughout the promoter CGIs of the juxtaposed transgenes (Supplemental Figures 2 and 3). These positive results prompted us to generate a mouse model with targeted knockin of the promethylation *cis* element at the *p16* locus.

We introduced the *cis* element approximately 1 kb upstream of the *p16* transcription start site (TSS) in mouse ES cells (mESCs)

Conflict of interest: The authors have declared that no conflict of interest exists.
Submitted: April 7, 2014; **Accepted:** June 5, 2014.
Reference information: *J Clin Invest*. 2014;124(9):3708–3712. doi:10.1172/JCI76507.

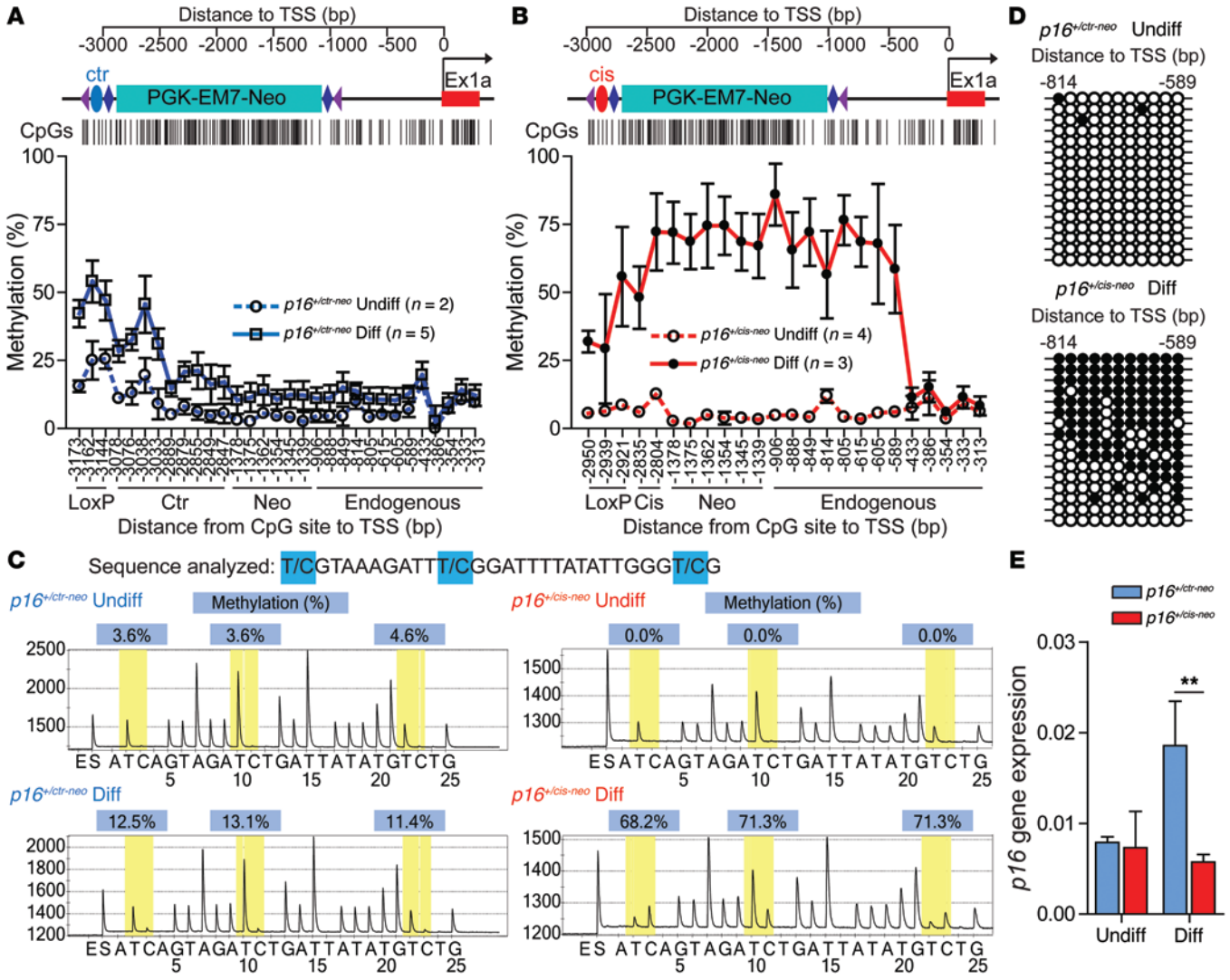

Figure 1. The *cis* element specifically induces p16 promoter methylation. Quantitative DNA methylation profiling in $p16^{+/ctr\text{-}neo}$ (**A**) and $p16^{+/cis\text{-}neo}$ (**B**) mESCs before (Undiff) and after (Diff) differentiation. Schematics of the *p16* promoter of targeted alleles, including CpG maps, are shown above. Ex1a, exon 1α. (**C**) Examples of bisulfite pyrograms of 3 CpG sites between –615 to –589 bp relative to TSS in $p16^{+/ctr\text{-}neo}$ and $p16^{+/cis\text{-}neo}$ mESCs before and after differentiation. The *y* axis represents the signal intensity of luminescence as a measure of nucleotide incorporation, and the *x* axis shows the dispensation order of nucleotide. CpG sites are shaded yellow, and the percentage methylation (blue boxes) was measured based on the signal intensities of C and T (representing methylated and unmethylated cytosines, respectively) in each C of a CpG site. (**D**) Clonal bisulfite sequencing analysis of 11 CpG sites (white, unmethylated; black, methylated) between –814 to –589 bp relative to TSS. Each row represents an individual clone. Whereas essentially no promoter methylation was observed in undifferentiated $p16^{+/cis\text{-}neo}$ mESCs, extensive methylation was found in differentiated $p16^{+/cis\text{-}neo}$ mESCs. (**E**) Quantitative *p16* gene expression analysis showed strong transcriptional suppression in differentiated $p16^{+/cis\text{-}neo}$ cells compared with controls. Values are mean ± SD. $^{**}P < 0.01$, Student's *t* test.

through homologous recombination (Supplemental Figure 4). The insertion leaves the *p16* core promoter intact and avoids affecting the $p15^{Ink4b}$, *p15* antisense (*p15AS*), and $p19^{Arf}$ promoters, located >27, >12, and >11 kb away, respectively (Supplemental Figure 4, A and B). As a negative control for insertion effects, we compared the effects of *cis* element against those of an *Alu* sequence located approximately 1 kb upstream of human *p16*, since this *Alu* shows no sequence homology to the *cis* element, and site-specific integration of this repetitive element does not affect methylation at neighboring genes (24). Germline transmission of both the control and *cis* elements was achieved and confirmed by Southern blotting, PCR, and DNA sequence analysis (Supplemental Figure 4, C and D).

To initially determine whether the knockin *cis* element specifically induces DNA methylation at the endogenous *p16* promoter, we studied mESCs in vitro. Differentiating ESCs recapitulate the earliest stages of embryonic lineage development. We therefore analyzed the progression of DNA methylation before and after induced differentiation (25, 26) in mESCs carrying either knockin allele. To characterize the dynamics of methylation establishment, we performed detailed methylation profiling by quantitative bisulfite pyrosequencing at CpG sites spanning the knockin sequence and the endogenous *p16* promoter (–906 to –313 bp relative to TSS). Prior to differentiation, this region was essentially unmethylated in both control ($p16^{+/ctr\text{-}neo}$) and *cis*-knockin ($p16^{+/cis\text{-}neo}$) mESCs (Figure 1, A–C). Upon differentiation of $p16^{+/ctr\text{-}neo}$ mESCs, a few CpG sites

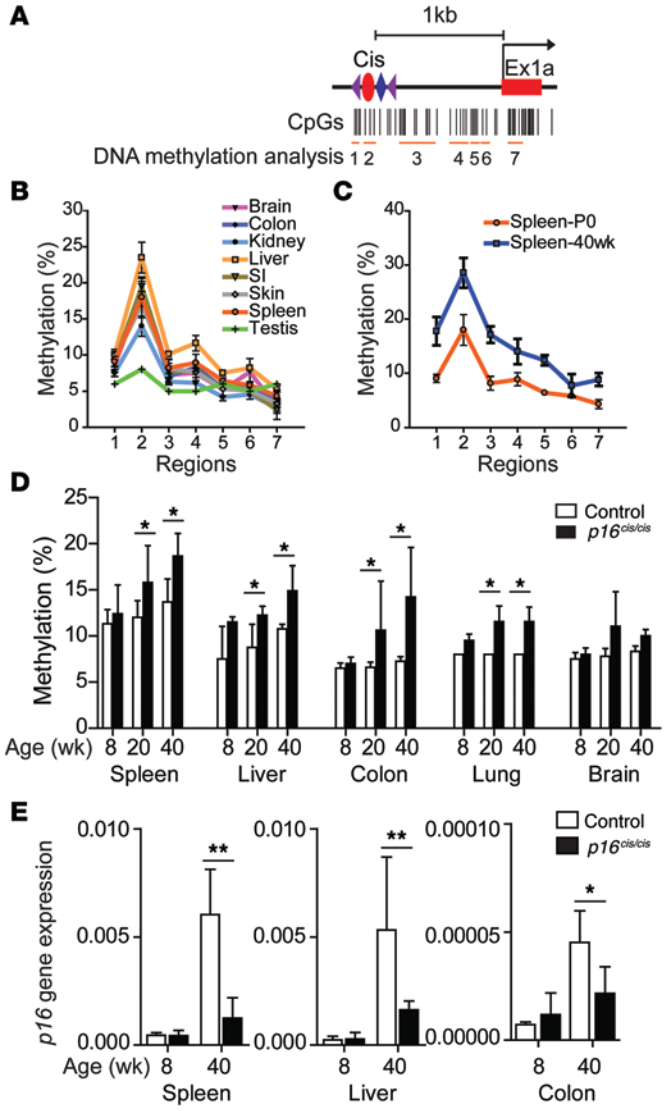

Figure 2. The *cis* element induces p16 promoter methylation and age-dependent transcriptional suppression in vivo. (**A**) CpG maps and regions assayed for DNA methylation. (**B**) DNA methylation profiling in multiple tissues from $p16^{cis/cis}$ mice (n = 2) at P0. (**C**) Comparison of methylation profiling in the spleens obtained from $p16^{cis/cis}$ mice at P0 and 40 weeks of age (n = 2–4 per time point). (**D**) Significant age-associated increases in DNA methylation in multiple tissues from $p16^{cis/cis}$ mice compared with controls (n = 3–4 per group). Shown are average methylation levels at promoter CpGs between −814 to −589 bp relative to TSS. (**E**) Significantly reduced *p16* mRNA levels in tissues from 40-week-old $p16^{cis/cis}$ mice compared with controls (n = 3–4 per group). Values are mean ± SD. $^*P < 0.05$, $^{**}P < 0.01$, Student's t test.

within the knockin sequence showed modestly increased methylation, but methylation remained low at the endogenous *p16* promoter (Figure 1, A and C). In $p16^{+/cis\text{-}neo}$ mESCs, conversely, differentiation induced dramatically increased methylation both at the *cis* element and at the *p16* promoter (Figure 1, B and C). These results clearly demonstrated that the *cis* element attracts de novo methylation during differentiation, also affecting neighboring endogenous sequence. Bisulfite cloning and sequencing, an independent method of assessing DNA methylation, confirmed the extensive developmentally regulated methylation in $p16^{+/cis\text{-}neo}$ mESCs (Figure 1D). Interestingly, methylation at the *cis*-targeted alleles exhibited clonal heterogeneity. Since our assay was designed to detect methylation at the targeted allele using a forward primer specific for the knockin sequence, our data suggest that the increased methylation occurs in a cell type–specific fashion. Finally, to monitor the functional effects of induced methylation, we assessed *p16* expression using quantitative TaqMan real-time RT-PCR. In $p16^{+/ctr\text{-}neo}$ cells, *p16* expression was upregulated during differentiation (Figure 1E), consistent with its functional role in limiting the replicative capacity of stem cells (27). In $p16^{+/cis\text{-}neo}$ cells, however, induced promoter methylation during differentiation led to strong transcriptional repression (Figure 1E). *p16* expression was restored by treatment with the DNA hypomethylating agent 5-aza-2′-deoxycytidine (DAC) (Supplemental Figure 5A), providing further validation that *p16* silencing is not due to unforeseen side effects of the *cis* element knockin. Importantly, consistent with previous studies (28, 29), we observed concomitant increases in repressive histone markers (H3K9me2 and H3K27me3), with no changes of active markers (H3K9Ac and H3K4me3), across the *p16* promoter (Supplemental Figure 5B), which suggests that *cis*-mediated epigenetic silencing could be mechanistically reinforced by changes in chromatin configuration.

Having verified that our engineered *cis* element specifically induced developmentally regulated promoter methylation and transcriptional silencing, we analyzed *p16* methylation in multiple tissues from $p16^{cis}$ homozygous ($p16^{cis/cis}$) mice after excision of the Frt-flanked selection marker (Figure 2A). $p16^{cis/cis}$ mice were viable and fertile and did not display any developmental abnormalities (Supplemental Figure 6). In agreement with our data in differentiating mESCs, we observed initial methylation seeding within the *cis* element in almost all mouse tissues at birth (P0) (Figure 2B). The notable exception was testis, in which we detected low methylation at all CpG sites. This was remarkably consistent with our previous observations, since the promoter CGIs with which the sequence motifs were originally associated are also highly methylated in most tissues, except testis and sperm (23). With aging, *cis* element–mediated methylation spread toward the endogenous *p16* promoter (Figure 2C). In spleen, liver, and colon, normal age-related increases in DNA methylation at the *p16* promoter were significantly accelerated by the *cis* element, with commensurate reductions in gene expression (Figure 2, D and E, and Supplemental Figure 7). Collectively, these results demonstrated that our approach successfully induced developmentally regulated somatic *p16* epimutation, leading to transcriptional repression in vivo.

To test whether *p16* promoter methylation predisposes animals to tumor development, we used heterozygous intercrossing to generate a cohort of $p16^{+/+}$, $p16^{+/cis}$, and $p16^{cis/cis}$ mice (on a mixed 129/C57 genetic background) and monitored tumor development and survival. In mice aged 35–100 weeks, spontaneous tumors developed in 0 of 18 $p16^{+/+}$ (0%), 3 of 51 $p16^{+/cis}$ (5%), and 6 of 22 $p16^{cis/cis}$ (27%; P = 0.02 vs. $p16^{+/+}$) mice. Of the 3 $p16^{+/cis}$ mice with spontaneous tumor development, 1 developed lymphoma and 2 developed sarcoma (Supplemental Figure 8, A–C). The malignancies in the 6 $p16^{cis/cis}$ mice were sarcoma (n = 3), lymphoma (n = 2), and lung adenocarcinoma (n = 1) (Figure 3A and Supplemental Figure 8, D–I). Given that p16 deficiency in many human cancers involves mutation of one allele and promoter hypermethylation of the other (30), we next assessed the cooperative tumorigenic effects of combined

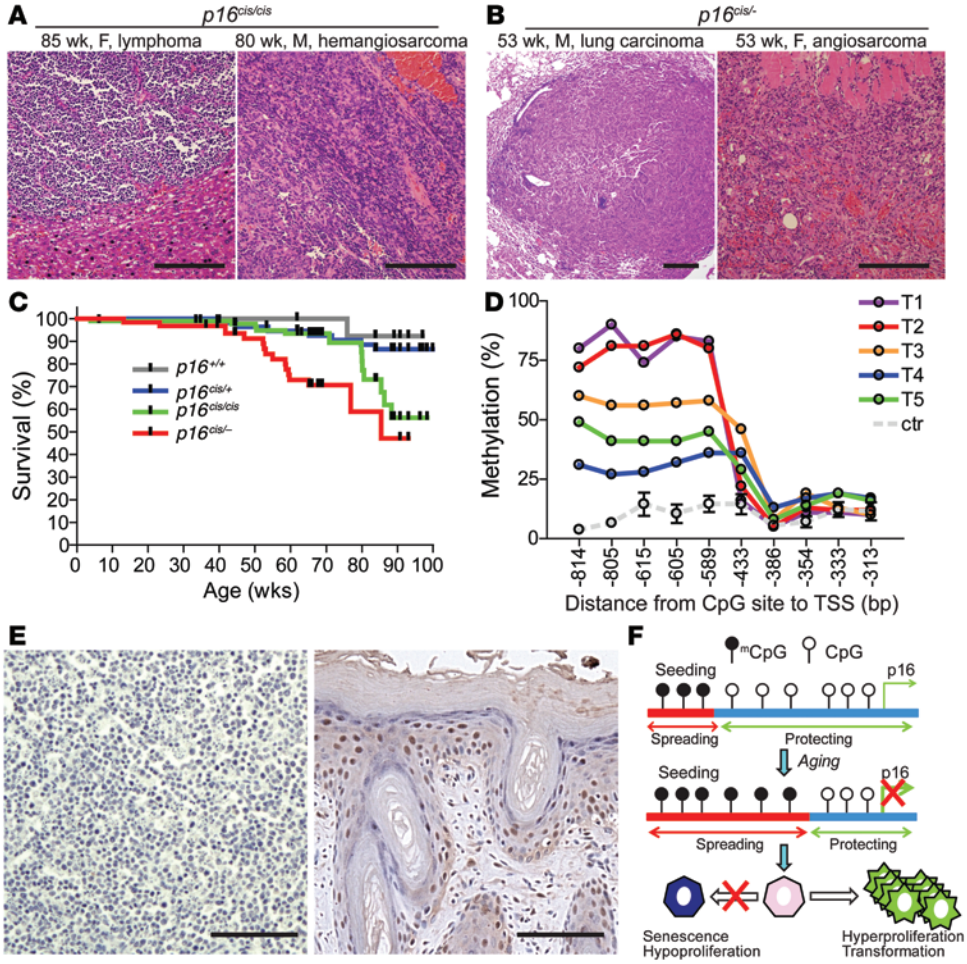

Figure 3. The driving role of p16 epimutation in tumorigenesis in vivo. (**A** and **B**) Representative histological appearance of malignancies in $p16^{cis/cis}$ (**A**) and $p16^{cis/-}$ (**B**) mice of the indicated age, sex, and tumor type. Scale bars: 200 μm. (**C**) Kaplan-Meier survival analysis demonstrating shortened lifespan in $p16^{cis/cis}$ mice ($P = 0.02$ vs. $p16^{+/+}$, log-rank test) and in $p16^{cis/-}$ mice. (**D**) *p16* promoter methylation significantly increased in the bulk of tumor tissues collected. Tumors 1 and 2 (T1 and T2) were collected from the liver and spleen, respectively, of the same $p16^{cis/cis}$ mouse with metastatic lymphoma; T3 was collected from the $p16^{+/cis}$ mouse; T4 and T5 were collected from 2 individual $p16^{cis/-}$ mice. Values for age-matched control tissues (ctr; mean ± SD, $n = 4$) are also shown. (**E**) Immunohistochemical analysis demonstrated that promoter hypermethylation resulted in abrogation of p16 protein expression in tumor cells. Left: Lymphoma with *p16* promoter hypermethylation. Right: Positive control skin tissue showing strong immunostaining. Scale bars: 100 μm. (**F**) Proposed model for a direct role of developmentally regulated *p16* methylation in tumorigenesis.

p16 mutation and epimutation. We bred the $p16^{cis}$ allele into mice on a *p16* exon 1α deletion background (31) to generate $p16^{cis/\Delta exon1\alpha}$ (mixed FVB/129/C57 background; referred to herein as $p16^{cis/-}$) mice. In 20 $p16^{cis/-}$ mice aged 40–91 weeks, 6 (30%) tumors were found; the malignancies were sarcoma ($n = 3$), lung carcinoma ($n = 2$), and lymphoma ($n = 1$) (Figure 3B and Supplemental Figure 9). Moreover, consistent with the notion of *p16* epimutation serving as 1 of Knudson's 2 hits, $p16^{cis/-}$ mice had accelerated tumor onset and shortened survival (Figure 3C). Our results compare favorably with previous studies that characterized the effects of *p16*-specific knockout on tumorigenesis (31, 32). Although rigorous comparisons in congenic strains have not yet been performed, the cancer-prone conditions in $p16^{cis/-}$ and $p16^{-/-}$ mice were strikingly similar: tumor spectra were predominantly sarcoma in both, tumor incidence was 30% and 35%, respectively, and tumor latency was 80 and 76 weeks, respectively. In contrast, $p16^{+/-}$ mice developed significantly fewer spontaneous tumors and exhibited significantly longer tumor-free survival. To ascertain the role of *p16* promoter methylation in the oncogenic pathway in vivo, we measured *p16* promoter methylation and gene expression in the tumor tissues. Hypermethylation of the *p16* promoter in tumors was associated with essentially complete loss of protein expression (Figure 3, D and E, and Supplemental Figures 10 and 11). Taken together, our results provide direct evidence for a driving role of *p16* epigenetic silencing by promoter hypermethylation in tumor formation and progression (Figure 3F).

In conclusion, our present study provides the first clear demonstration that *p16* epimutation causes tumorigenesis. Potential applications of this novel mouse model include the testing of targeted epigenetic therapies for prevention and treatment of human cancer. Our straightforward approach to epigenetic engineering should be useful in testing the causal role of other epigenetic alterations implicated in carcinogenesis, and broadly applicable toward elucidating epigenetic etiology in a wide range of diseases.

Methods

Further information can be found in Supplemental Methods and Supplemental Tables 1–3.

Statistics. 2-tailed Student's *t* test and Fisher exact test were used to determine the significance of differences. Survival analysis was conducted with Kaplan-Meier analysis and log-rank test. A *P* value less than 0.05 was considered significant.

Study approval. All animals were treated in accordance with NIH guidelines as approved by the Baylor College of Medicine Animal Care committee.

Acknowledgments

We thank Wei Zhu, Wei Wei, and Jingming Shu for technical assistance and Adam Gillum for assistance with the figures. We acknowledge the shared resources by Baylor College of Medicine ESC and GEM cores (NIH/NCI grant P30CA125123) and by Morphology core at the Texas Medical Center Digestive Disease Center (NIH/NIDDK grant P30DK56338). This work was supported by grants from the Sidney Kimmel Foundation

(to L. Shen), USDA (CRIS-6250-51000-055 to L. Shen and R.A. Waterland; CRIS-6250-51000-054 to M.H. Chen), March of Dimes (1-FY-08-392 to R.A. Waterland), and NIDDK (1R01DK081557 to R.A. Waterland).

Address correspondence to: Lanlan Shen, Department of Pediatrics, Baylor College of Medicine, USDA/ARS Children's Nutrition Research Center, 1100 Bates St., Ste. 8020, Houston, Texas 77030, USA. Phone: 713.798.0317; E-mail: Lanlan.Shen@bcm.edu.

1. Holliday R. The inheritance of epigenetic defects. *Science*. 1987;238(4824):163–170.
2. Feinberg AP, Tycko B. The history of cancer epigenetics. *Nat Rev Cancer*. 2004;4(2):143–153.
3. Baylin SB, Jones PA. A decade of exploring the cancer epigenome — biological and translational implications. *Nat Rev Cancer*. 2011;11(10):726–734.
4. Shen L, et al. DNA methylation and environmental exposures in human hepatocellular carcinoma. *J Natl Cancer Inst*. 2002;94(10):755–761.
5. Shen L, et al. Integrated genetic and epigenetic analysis identifies three different subclasses of colon cancer. *Proc Natl Acad Sci U S A*. 2007;104(47):18654–18659.
6. Shen L, et al. Association between DNA methylation and shortened survival in patients with advanced colorectal cancer treated with 5-fluorouracil based chemotherapy. *Clin Cancer Res*. 2007;13(20):6093–6098.
7. Shen L, et al. DNA methylation predicts survival and response to therapy in patients with myelodysplastic syndromes. *J Clin Oncol*. 2010;28(4):605–613.
8. Baylin S, Bestor TH. Altered methylation patterns in cancer cell genomes: cause or consequence? *Cancer Cell*. 2002;1(4):299–305.
9. Laird PW. The power and the promise of DNA methylation markers. *Nat Rev Cancer*. 2003;3(4):253–266.
10. Issa JP, Ottaviano YL, Celano P, Hamilton SR, Davidson NE, Baylin SB. Methylation of the oestrogen receptor CpG island links ageing and neoplasia in human colon. *Nat Genet*. 1994;7(4):536–540.
11. Sharpless NE, DePinho RA. The INK4A/ARF locus and its two gene products. *Curr Opin Genet Dev*. 1999;9(1):22–30.
12. Herman JG, et al. Inactivation of the CDKN2/p16/MTS1 gene is frequently associated with aberrant DNA methylation in all common human cancers. *Cancer Res*. 1995;55(20):4525–4530.
13. Issa JP, Ahuja N, Toyota M, Bronner MP, Brentnall TA. Accelerated age-related CpG island methylation in ulcerative colitis. *Cancer Res*. 2001;61(9):3573–3577.
14. Kondo Y, Kanai Y, Sakamoto M, Mizokami M, Ueda R, Hirohashi S. Genetic instability and aberrant DNA methylation in chronic hepatitis and cirrhosis — a comprehensive study of loss of heterozygosity and microsatellite instability at 39 loci and DNA hypermethylation on 8 CpG islands in microdissected specimens from patients with hepatocellular carcinoma. *Hepatology*. 2000;32(5):970–979.
15. Nuovo GJ, Plaia TW, Belinsky SA, Baylin SB, Herman JG. In situ detection of the hypermethylation-induced inactivation of the p16 gene as an early event in oncogenesis. *Proc Natl Acad Sci U S A*. 1999;96(22):12754–12759.
16. Belinsky SA, et al. Aberrant methylation of p16(INK4a) is an early event in lung cancer and a potential biomarker for early diagnosis. *Proc Natl Acad Sci U S A*. 1998;95(20):11891–11896.
17. Maegawa S, et al. Widespread and tissue specific age-related DNA methylation changes in mice. *Genome Res*. 2010;20(3):332–340.
18. Nishida N, Nagasaka T, Nishimura T, Ikai I, Boland CR, Goel A. Aberrant methylation of multiple tumor suppressor genes in aging liver, chronic hepatitis, and hepatocellular carcinoma. *Hepatology*. 2008;47(3):908–918.
19. Waki T, Tamura G, Tsuchiya T, Sato K, Nishizuka S, Motoyama T. Promoter methylation status of E-cadherin, hMLH1, and p16 genes in nonneoplastic gastric epithelia. *Am J Pathol*. 2002;161(2):399–403.
20. Baylin SB, Ohm JE. Epigenetic gene silencing in cancer - a mechanism for early oncogenic pathway addiction? *Nat Rev Cancer*. 2006;6(2):107–116.
21. Lienert F, Wirbelauer C, Som I, Dean A, Mohn F, Schübeler D. Identification of genetic elements that autonomously determine DNA methylation states. *Nat Genet*. 2011;43(11):1091–1097.
22. Yates PA, Burman RW, Mummaneni P, Krussel S, Turker MS. Tandem B1 elements located in a mouse methylation center provide a target for de novo DNA methylation. *J Biol Chem*. 1999;274(51):36357–36361.
23. Shen L, et al. Genome-wide profiling of DNA methylation reveals a class of normally methylated CpG island promoters. *PLoS Genet*. 2007;3(10):2023–2036.
24. Zhang Y, Shu J, Si J, Shen L, Estecio MR, Issa JP. Repetitive elements and enforced transcriptional repression co-operate to enhance DNA methylation spreading into a promoter CpG-island. *Nucleic Acids Res*. 2012;40(15):7257–7268.
25. Bibel M, Richter J, Lacroix E, Barde YA. Generation of a defined and uniform population of CNS progenitors and neurons from mouse embryonic stem cells. *Nat Protoc*. 2007;2(5):1034–1043.
26. McKinney-Freeman S, Daley G. Derivation of hematopoietic stem cells from murine embryonic stem cells. *J Vis Exp*. 2007;(2):162.
27. Li H, et al. The Ink4/Arf locus is a barrier for iPS cell reprogramming. *Nature*. 2009;460(7259):1136–1139.
28. Esteve PO, et al. Direct interaction between DNMT1 and G9a coordinates DNA and histone methylation during replication. *Genes Dev*. 2006;20(22):3089–3103.
29. Yamakoshi K, et al. Real-time in vivo imaging of p16Ink4a reveals cross talk with p53. *J Cell Biol*. 2009;186(3):393–407.
30. Rocco JW, Sidransky D. p16(MTS-1/CDKN2/INK4a) in cancer progression. *Exp Cell Res*. 2001;264(1):42–55.
31. Sharpless NE, et al. Loss of p16Ink4a with retention of p19Arf predisposes mice to tumorigenesis. *Nature*. 2001;413(6851):86–91.
32. Sharpless NE, Ramsey MR, Balasubramanian P, Castrillon DH, DePinho RA. The differential impact of p16(INK4a) or p19(ARF) deficiency on cell growth and tumorigenesis. *Oncogene*. 2004;23(2):379–385.